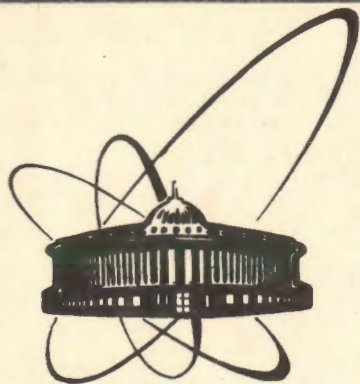


90-277

+



СООБЩЕНИЯ
ОБЪЕДИНЕННОГО
ИНСТИТУТА
ЯДЕРНЫХ
ИССЛЕДОВАНИЙ
ДУБНА

S-67

E1-90-277

B. Słowiński

ELECTROMAGNETIC CASCADES PRODUCED
BY GAMMA-QUANTA WITH THE ENERGY

$E_{\gamma} = 100-3500$ MeV

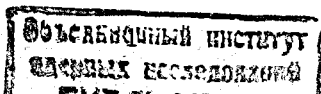
VI. General Features

1990

I. INTRODUCTION

In recent years the knowledge of an electromagnetic cascade process (ECP or e.m. shower) induced by high energy gamma-quanta (GQ) in dense enough media, which is of special interest from practical point of view, comes to the explicit, compact and reliable information about main characteristics of the process such as longitudinal and lateral profile, as well as their correlations and relevant fluctuations. Nevertheless, little experimental data on e.m. showers is available in the literature while the published ones are mainly fragmentary, aiming, for example, to carry out a calibration of electromagnetic calorimeters, etc. On the other hand, existing Monte Carlo computer programs of ECP simulation^{1,2/} being in principle universal and exhaustive are rather embarrassing in practical usage although a three-dimensional parametrization of appropriate data was obtained^{3/}. Therefore, a systematic and extensive experimental investigation of the ECP created by GQ of energy between 100 and 3500 MeV has been performed using pictures of the 180 l xenon bubble chamber (XeBC) of ITEP (Moscow)^{4/}. This chamber having large enough dimensions expressed in units of radiation length (r.l.) equal to $25.7 \times 11 \times 10$ r.l.³, and providing an acceptably clear image of electron tracks of energy not less than 0.5-1.5 MeV enables it to measure practically all ranges of shower electrons and positrons (later: electrons) registered in a picture plane (PP). Consequently it turns out possible a thorough analysis of such complicated process without any substantial distortion caused by the detector effect, may be, a relatively small, along the shower axis (SA), $\Delta t = 2$ r.l., and thin ($\Delta p = 0.25$ r.l.) region very close to the shower maximum nearby the SA at higher energies (i.e. at $E_\gamma \geq 1500$ MeV) where the density of electrons becomes sometimes too large to separate some overlapping short electron tracks.

This work is the last one in a series^{5-9/} summarizing our previously obtained results concerning the longitudinal and the transversal development of e.m. showers within the sufficiently wide interval of primary GQ energy $E_\gamma = 100-3500$ MeV. These results include as well the longitudinal-lateral correlations and the fluctuations. The measured ECP characteristics are summary plane projection ranges of shower



electrons (SER), observed inside a rectangle with the dimensions of $\Delta t = 0.6$ r.l. along the SA and $\Delta p = 0.3$ r.l. in its lateral direction^{5/}, the shower depth t being measured from the conversion point of a primary GQ. As has been shown earlier^{10/} the SER multiplied by some constant value $\eta = 3.63$ MeV/mm are appropriately, i.e. on the average and to within $\sim 3\%$, equal to their ionization loss (IL) at least in the central e.m. shower region where more than 90% of the total IL of shower electrons is released. Mention finally that the total number of e.m. shower events fulfilling the appropriate criteria^{5/} equals 908 and they were grouped into 22 bins of primary GQ energy^{5/} in such a way that the relative width $\Delta E_\gamma / E_\gamma \approx 0.1$ don't exceed the energy resolution of GQ in the XeBC.

II. LONGITUDINAL PROFILE

The longitudinal distribution of shower electron IL is displayed in fig.1 for six among 22 analysed in the work intervals of energy E_γ of e.m. showers initiating GQ. As has been found out^{6/} the experimental data may be parametrized by the Weibull function shown in the figure as smooth lines. But simple inspection of fig.1 indicates that this function, being acceptable as far as IL of shower electrons falls below $\sim 1\%$ of the total IL, is in bad response to the long tail of experimental distribution suggesting rather its exponential behaviour which may be well described by a gamma function.

Figure 2 presents the cumulative longitudinal distribution of IL for six values of energy E_γ as a function of the dimension-free ratio $t/\bar{t}(E_\gamma)$, where $\bar{t}(E_\gamma)$ is the average value of the length t . Its energy dependence is illustrated in fig.3 and fitted to the linear function of $\ln E_\gamma$:

$$\bar{t}(E_\gamma) = a_t + b_t \cdot \ln E_\gamma \quad (1)$$

also shown in the figure as a solid line. Here $a_t = -4.84 \pm 0.09$, $b_t = 1.32 \pm 0.03$ at the linear correlation index $r=0.996$, when \bar{t} is in r.l. and E_γ is in MeV. One can notice that at $E_\gamma \geq 1000$ MeV the distribution becomes independent of the energy E_γ . So, the average length \bar{t} is useful scaling parameter for longitudinal development of the ECP generalizing a description of its longitudinal IL deposition profile.

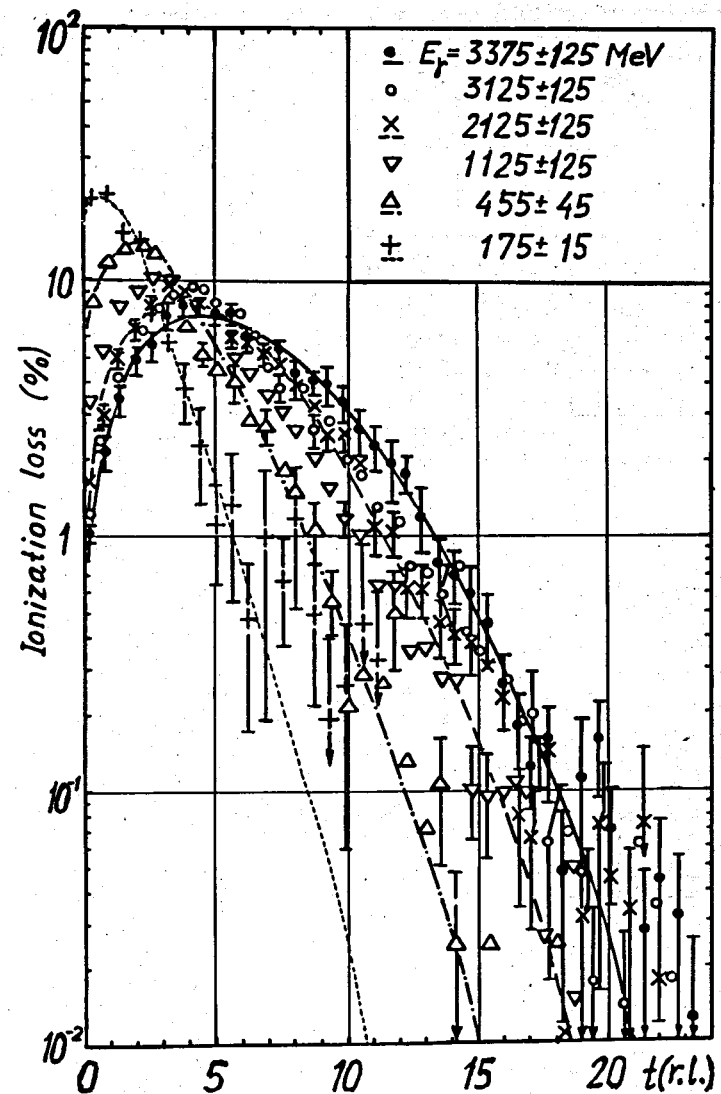


Fig. 1. Longitudinal distribution of average ionization loss in e.m. showers produced by GQ with the energy E_γ in liquid xenon. The length t is in units of radiation length. Curves designate the fit to the Weibull function.

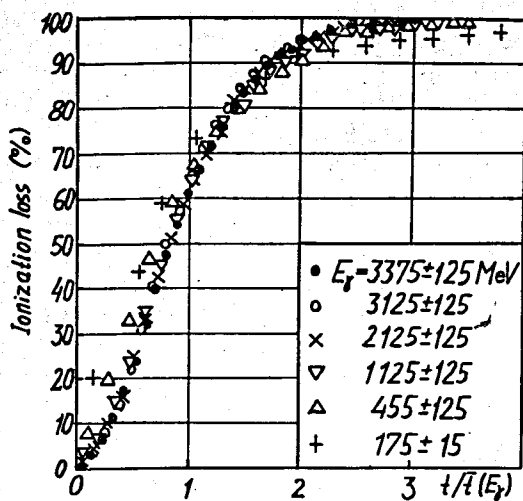


Fig. 2. Cumulative longitudinal distribution of average ionization loss in e.m. showers produced by GQ with the energy E_γ in liquid xenon; $t/\bar{t}(E_\gamma)$ is the dimension-free ratio of the shower length t and the average shower length $\bar{t}(E_\gamma)$ at the energy E_γ .

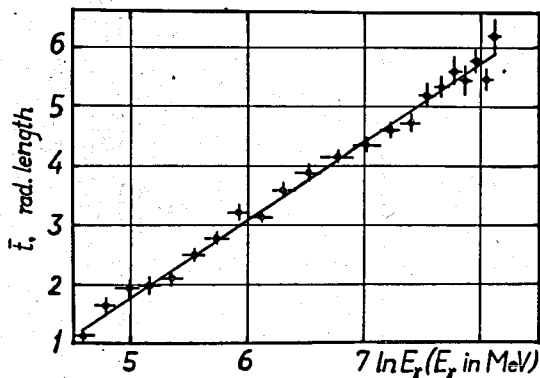


Fig. 3. The average shower length t as a function of the energy E_γ of primary photons. Superimposed is the fitting function^{11/}.

III. LATERAL PROFILE

As pointed out earlier the 180 l XeBC used in the work as a detector of high energy GQ enables it to obtain the experimental information about the lateral IL profile in a projection plane whereas the relevant average radial IL distribution can be reconstructed taking into account the geometric conditions of the shower electron ranges recording in the PP, as well as axial symmetry of the IL around the SA, if averaged over all fluctuations^{7/}. Figure 4 shows the average lateral IL distribution summed over all depth t as a function of the distance p measured from the SA in the PP for seven values of energy E_γ . The same distribution but vs. the ratio $p/\bar{p}(E_\gamma)$

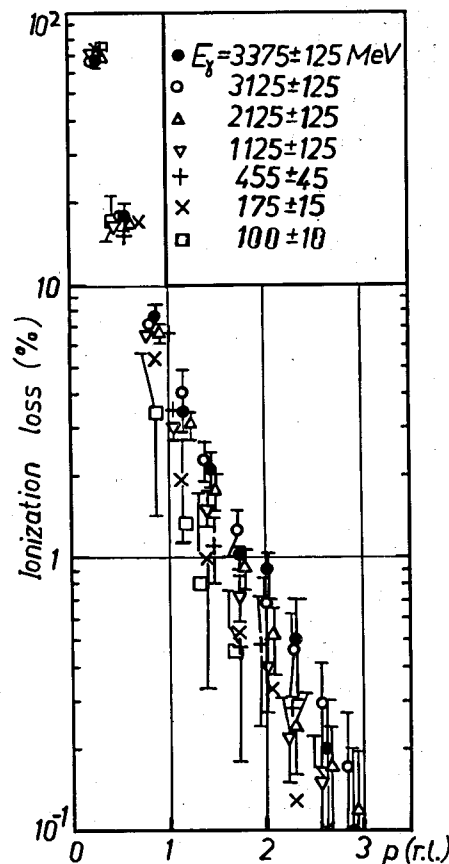


Fig. 4. Lateral distribution of average ionization loss in e.m. showers produced by GQ with the energy E_γ in liquid xenon; p is the distance from the shower axis measured in the picture plane.

is plotted in fig. 5. Here $\bar{p}(E_\gamma)$ is the average value of p at a given energy E_γ . The energy dependence of $\bar{p}(E_\gamma)$ was fitted to the simple linear function of $\ln E_\gamma$ as

$$\bar{p}(E_\gamma) = a_p + b_p \cdot \ln E_\gamma \quad (2)$$

with $a_p = 0.21 \pm 0.03$, $b_p = 0.058 \pm 0.005$ and the linear correlation index $r=0.93$. Relevant experimental data and the fitted linear regression^{12/} are presented in fig. 6. One can see that at $E_\gamma \geq 500$ MeV the plane average lateral IL distribution scaled in $\bar{p}(E_\gamma)$ is independent of E_γ (fig. 5) similarly as in the case of the cumulative longitudinal IL distribution (fig. 2).

The lateral average IL distribution $f(p|t, E_\gamma)$ in the PP at any fixed shower depth t has been found^{7/} exponentially dependent on p as

$$f(p|t, E_\gamma) = \frac{1}{\bar{p}_0(t, E_\gamma)} \cdot e^{-p/\bar{p}_0(t, E_\gamma)} \quad (3)$$

when normalized to unity. The slope parameter $\bar{p}_0(t, E_\gamma)$ may be fitted to the linear function of t and $\ln E_\gamma$ ^{7/}. Corresponding radial spread of the IL, $F(r|t, E_\gamma)$, is to be obtained as a solution of the integral equation^{7/}:

$$f(p|t, E_\gamma) = 2 \int_p^\infty \frac{F(r|t, E_\gamma) dr}{\sqrt{1-(p/r)^2}} \quad (4)$$

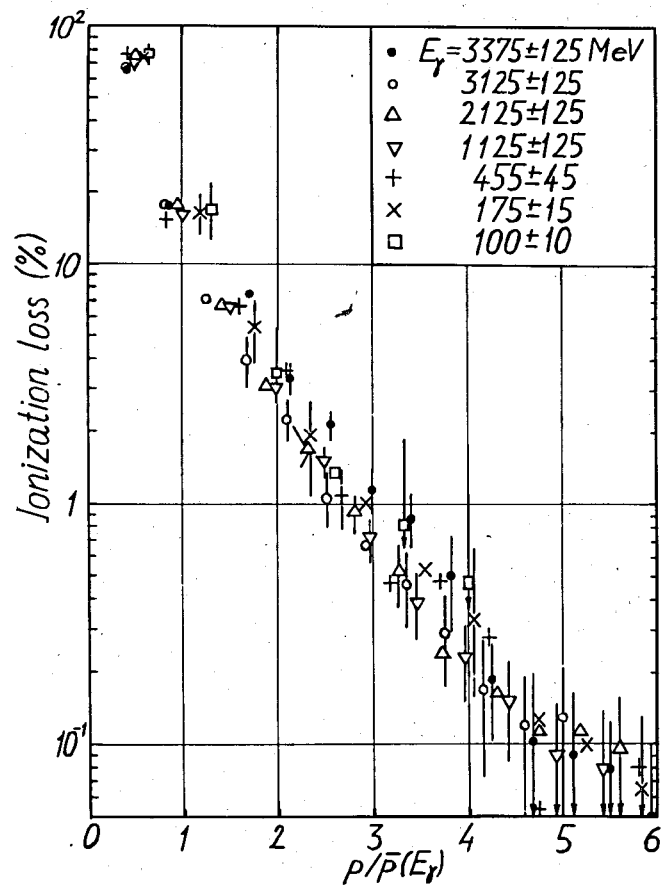


Fig. 5. Same as fig. 4 but vs. the dimension-free ratio of the distance p from the shower axis measured in the picture plane and the average lateral width $\bar{p}(E_\gamma)$.

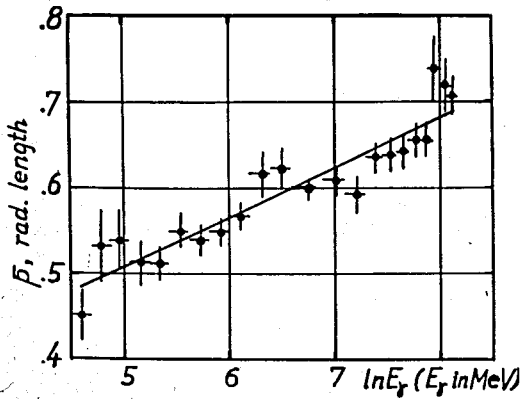


Fig. 6. The average lateral width \bar{p} as a function of the energy E_γ of primary GQ. The straight line shows the best fit to the linear function of $\ln E_\gamma$.

following from the geometrical conditions of the shower electron tracks registration in the XeBC pictures.

IV. CORRELATION

The experimental material used in the work makes it possible to study the correlation between such coordinates (t, p) that inside the volume of liquid xenon limited by two parallel planes each distant from the SA by p and the plane at the depth t along the SA the part A of the total shower electron IL is deposited when the conversion point of a primary shower initiating photon is at $t = 0$. Figure 7 presents the aforesaid (t, p) dependence averaged over all fluctuations for

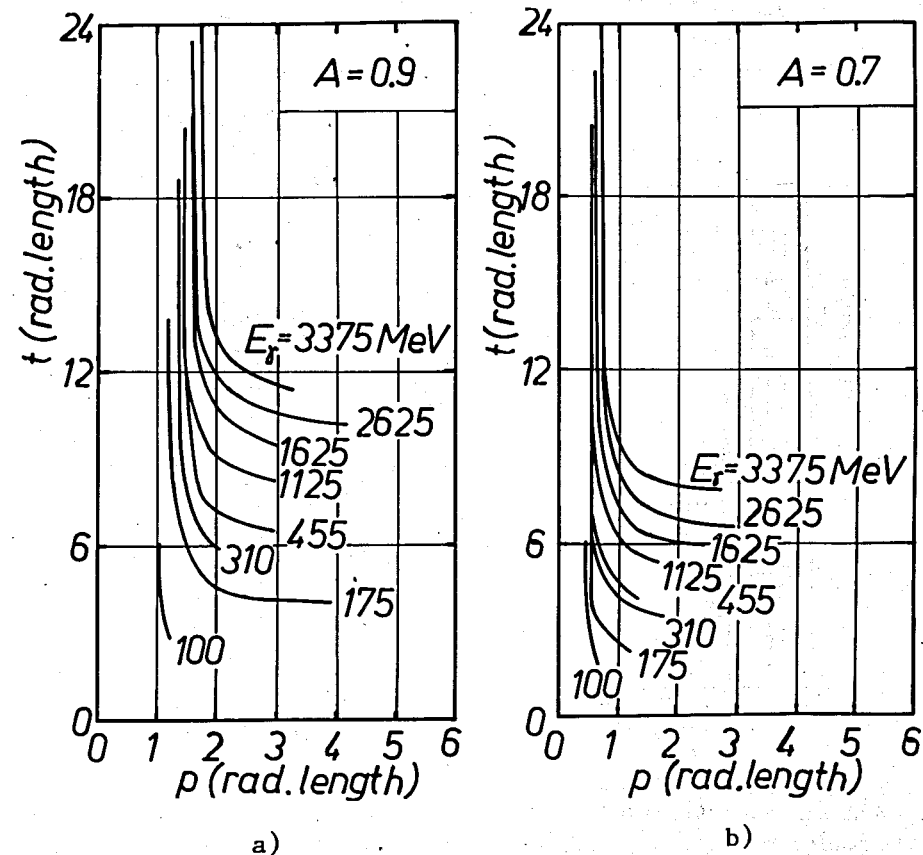


Fig. 7. The average shower length t vs. the average shower width p for the part $A=0.9$ and 0.7 of the total ionization loss at different values of the energy E_γ of primary GQ initiating showers.

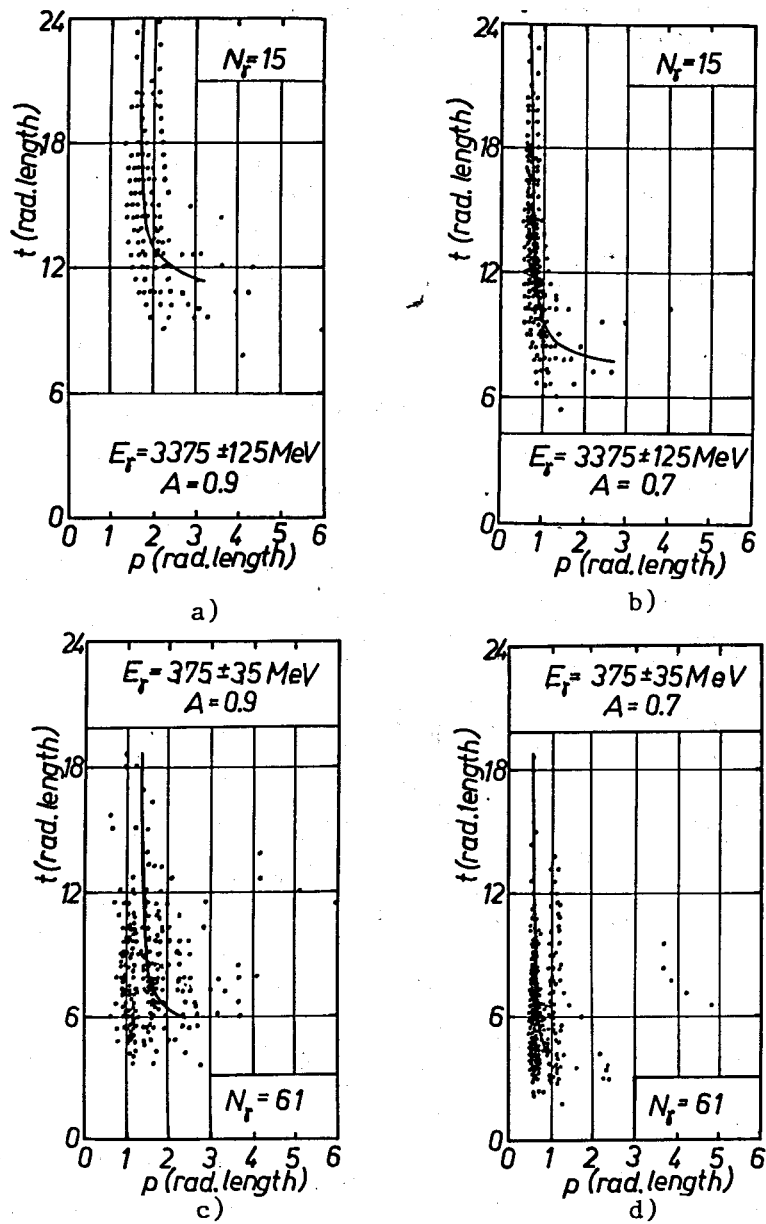


Fig. 8. Scatter plot of the shower length t vs. the shower width p for two different parts $A=0.9$ and 0.7 of the total ionization loss at two values of the energy $E_\gamma = 3375 \text{ MeV}$ and 375 MeV of primary photons. Solid lines indicate the relative average dependences. N_γ is the number of GQ events including in the appropriate interval of energy E_γ .

8 intervals of energy E_γ and two values of A : 0.9 and 0.7 . How much may be the relevant fluctuations at different E_γ and A is illustrated in fig.8 where (t, p) scatter plots are displayed for two remote values of energy E_γ : 3375 and 375 MeV , as well as two above values of A . In more detail this problem is discussed and experimentally argued in^{8/}.

V. FLUCTUATIONS

1. Internal Structure

Figure 9 shows the standard deviation (SD) $\sigma_A^{(t)}$ of a part A of the IL deposited along the SA as a function of A for six values of energy E_γ of shower initiating GQ. One can notice

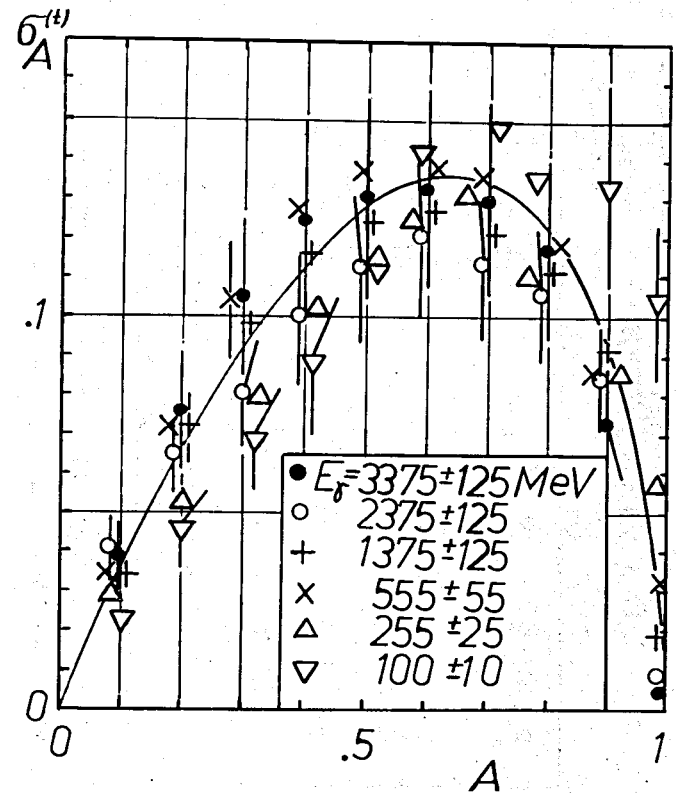


Fig. 9. Longitudinal standard deviation $\sigma_A^{(t)}$ of the part A of the ionization loss deposited along the shower axis for different values of the energy E_γ of primary GQ. Solid lines display the fit to the form $1/5$.

that at $E_\gamma \geq 500$ MeV the behavior of $\sigma_A^{(t)}$ with A is independent of the energy E_γ , within the error. It was parametrized by a simple parabolic function¹⁷⁾:

$$\sigma_A^{(t)} = A(\sqrt{\alpha_t^2 + \beta_t(\gamma_t - A)} - \alpha_t) \quad (5)$$

with $\alpha_t = 0.038 \pm 0.001$, $\beta_t = 0.166 \pm 0.005$, $\gamma_t = 1.01 \pm 0.01$, which is illustrated in the figure by the solid curve.

The lateral IL fluctuations may be characterized by the A dependence of the SD $\sigma_A^{(p)}$ of the part A of the IL measured in the PP as released in the lateral direction away from the SA. Relevant experimental data normalized to the maximum value $(\sigma_A^{(p)})_{\max}$ of $\sigma_A^{(p)}$ are displayed in fig. 10 for the same energy as earlier (fig.9) six values of energy E_γ . The energy dependence of $(\sigma_A^{(p)})_{\max}$ was fitted to the linear function of $\ln E$ as

$$(\sigma_A^{(p)} / A)_{\max} = a_p - \beta_p \ln E_\gamma \quad (6)$$

with $a_p = 0.48 \pm 0.02$, $\beta_p = 0.048 \pm 0.003$ and the correlation coefficient = 0.95.

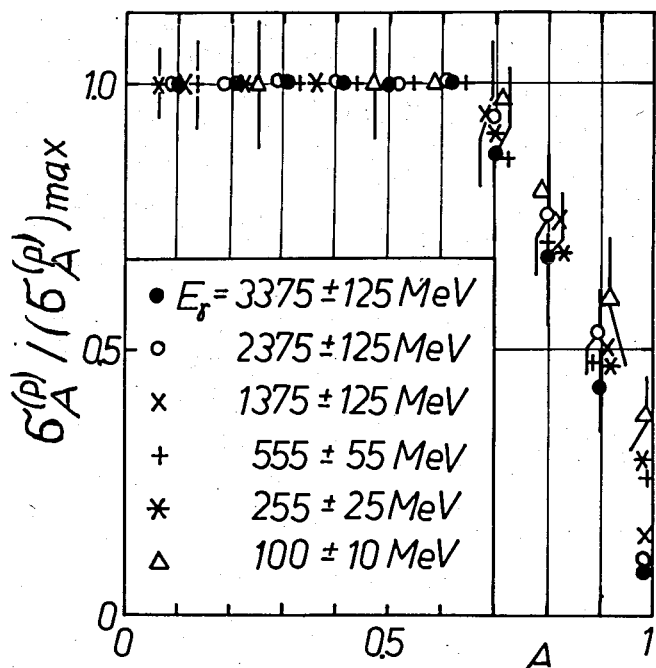


Fig. 10. Similar as fig.9 but for the lateral standard deviation $\sigma_A^{(p)}$ normalized to the maximum value $(\sigma_A^{(p)})_{\max}$ of $\sigma_A^{(p)}$.

2. Geometric Shape

The longitudinal and transversal e.m. shower shape diffuseness may be described by the corresponding coefficients of variation S_t/\bar{t} and S_p/\bar{p} which are plotted in fig.11 for all 22 intervals of energy E_γ of shower initiating GQ. Their energy dependence was parametrized by linear functions of $\ln E_\gamma$ as

$$S_t/\bar{t} = A_t - B_t \cdot \ln E_\gamma \quad \text{and} \quad S_p/\bar{p} = A_p - B_p \cdot \ln E_\gamma, \quad (7)$$

where $A_t = 0.61 \pm 0.02$, $B_t = (5.8 \pm 0.1) \cdot 10^{-2}$, $r = 0.90$, and $A_p = 3.38 \pm 0.04$, $B_p = (3.3 \pm 0.1) \cdot 10^{-2}$, $r = 0.95$. They are shown in the figure as straight lines.

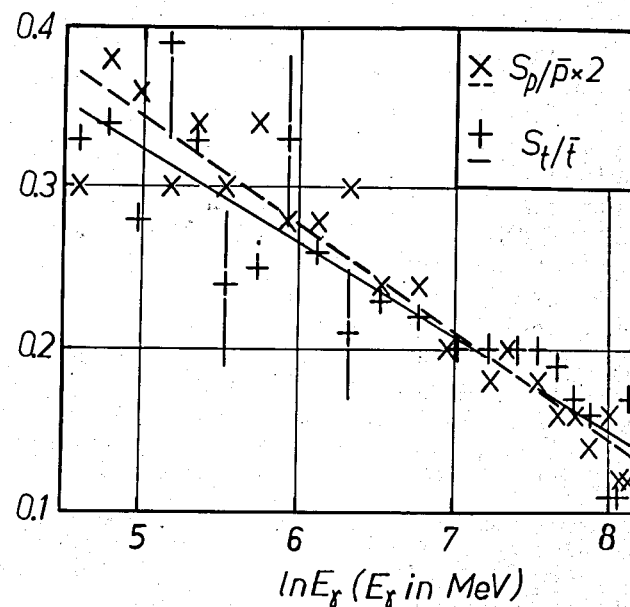


Fig.11. Coefficients of variation of the longitudinal S_t/\bar{t} and the lateral S_p/\bar{p} shower dimensions. Straight lines present the best fits to linear functions¹⁷⁾.

VI. CONCLUSIONS

A systematic experimental study of e.m. showers produced by GQ of energy $E_\gamma = 100-3500$ MeV in liquid xenon has been carried out using the pictures of the 180 l XeBC of ITEP (Moscow) exposed to the beam of π^- mesons at 3.5 GeV/c. The results are as follows:

1. The longitudinal distribution of average ionization loss of shower electrons was satisfactorily fitted to the Weibull function, at least up to shower depths t at which the IL falls to about 1% (fig. 1). The cumulative IL distribution scaled in the average shower depth $\bar{t}(E_\gamma)$ is independent of the energy E_γ at $E_\gamma \geq 500$ MeV (fig.2).

2. The transversal distribution of average IL, determined as released within two parallel planes each being parallel to the shower axis too and remote from it by a distance p , displays a simple scaling with the primary GQ energy E_γ when expressed in units of average values $\bar{p}(E_\gamma)$ of p (fig.5).

3. Average values of the depth t and the width $2 \cdot p$ of a box formed by two parallel planes with the SA in the middle and two other parallel planes perpendicular to the SA and separated a distance t (the part $A = 0.6-0.9$ of the total IL of shower electrons is deposited (on the average)) reveal a strong correlation within a small interval of $p \approx 1-2$ r.l. only at all energies E_γ (fig.7). Nevertheless, the relevant fluctuations are very large in this interval (fig.8).

4. Longitudinal fluctuations $\sigma_A^{(t)}$ of a part A of the total IL have been parametrized by a simple function of A which is independent of the energy E_γ at $E_\gamma \geq 500$ MeV (fig.9). Similar fluctuations $\sigma_A^{(p)}$ in the transversal to the SA direction as a function of A also displays an approximate scaling with the primary GQ energy E_γ when normalized to the maximum value of $(\sigma_A^{(p)})_{\max}$ (fig.10) which decreases with increasing energy E_γ as $\ln E_\gamma^{1/8}$. The coefficients of variation S_t/\bar{t} and S_p/\bar{p} linearly diminish with increasing $\ln E_\gamma$ (fig.11) indicating that the outer shape of e.m. showers becomes, on the average, relatively more distinct at higher energy E_γ .

REFERENCES

1. Nelson W.R., Hirayama H., Rogers D.W.O. - The EGS4 Code System, SLAC-265 (December 1985).
2. Brun R. et al. - GEANT User's Guide, CERN DD(EE) 84-1.
3. DeAngelis A. - NIM, 1988, A271, p.455.
4. Kuznetsov E.V. et al. - PTE 1970, 2, p.56 (in Russian).
5. Słowiński B. - JINR, E1-89-658, Dubna, 1989.
6. Słowiński B. - JINR, E1-89-676, Dubna, 1989.
7. Słowiński B. - JINR, E1-89-789, Dubna, 1989.
8. Słowiński B. - JINR, E1-90-273, Dubna, 1990.
9. Słowiński B. - JINR, E1-90-274, Dubna, 1990.
10. Słowiński B., Czyżewska D. - JINR, P13-88-239, Dubna, 1988.

Received by Publishing Department
on April 19, 1990.